36th Conference on

OUR WORLD IN CONCRETE & STRUCTURES

14 – 16 August 2011, Singapore

Conference Theme:
"Recent Advances in the Technology of Fresh Concrete"

Conference Documentation
Volume XXX

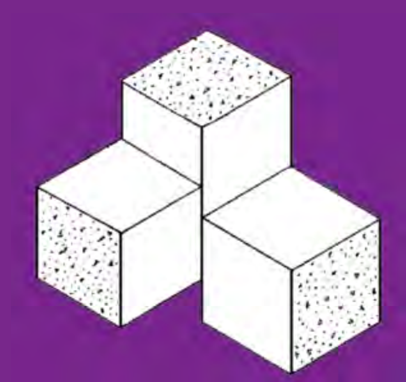

Conference Co-sponsors:

- BASF South East Asia Pte Ltd (*gold*)
- WAK Technologies Pte Ltd (*gold*)
- Unibeton Ready Mix, UAE
- Novaars International Pte Ltd
- Ready-Mixed Concrete Assn of Singapore
- Cement and Concrete Assn of Singapore
- Japan Concrete Institute

Organisers:

- CI-Premier Conference Organisation, Singapore

36th Conference on

Our World in Concrete & Structures

OWICS 2011 Conference Advisors

- Mr David Ball, UK
- Dr O Wallevik, Iceland
- Prof V Ramakrishnan, USA
- Dr C C Chang, USA
- Prof M C Tandon, India
- Mr R Sundaram, India
- Prof K Carter, USA
- Prof Issam Harik, USA
- Prof H Wallbaum, Switzerland
- Prof Mario Collepardi, Italy
- Mr Michael Khrapko, New Zealand
- Mr Chung-Ming Ho, Taiwan

OWICS 2011 Conference Committee

Conference Chairpersons:	A/Prof K C Gary Ong, NUS, Singapore
	A/Prof Min-Hong Zhang, NUS, Singapore
Co-ordinator:	Mr Yogesh Chhabra, Novaars International Pte Ltd
Conference Director:	Er John S Y Tan, CI-Premier Conference Organisation
Secretary:	Ms Peggy L P Teo, CONLOG
IT Manager:	Ms Amanda Quek, Singapore

The OWICS Steering Council

OWICS Honorary Emeritus Chairmen

- Em Prof S L Lee, Singapore
- Dr C T Tam, Singapore

OWICS Honorary Chairmen

- Prof Franco Mola, Italy
- Prof G M Sabnis, USA
- Prof Shoji Ikeda, Japan
- Mr C R Alimchandani, India
- Mr Chris Stanley, UAE
- Prof N Otsuki, Japan

OWICS Advisors

- Yukio Aoyagi, Japan
- Ken Day, Australia
- Willie Kay, Singapore
- Robert G Lee, USA
- Hoe-Peng Lim, Singapore
- Steven Loh, Singapore
- Kiat-Huat Seow, Singapore
- Teng-Hooi Tan, Singapore
- Petr Prochazka, Czech Republic
- JiaBiao Jiang, Singapore
- Desmond King, UK
- Ryoji Sakurada, Japan
- Gary K C Ong, Singapore

OWICS Corporate Advisors

- W R Grace Singapore Pte Ltd
- BASF South East Asia Pte Ltd

OWICS Organisation Advisors

- Ready-Mixed Concrete Association of Singapore
- American Concrete Institute-Singapore Chapter
- Singapore Concrete Institute
- Prestressed & Precast Concrete Society
- Cement and Concrete Association of Singapore
- Japan Concrete Institute
- Indian Concrete Institute

Proceedings of the 36th Conference on

OUR WORLD IN CONCRETE & STRUCTURES

14- 16 August 2011, Singapore

Theme: ***"Recent Advances in the Technology of Fresh Concrete"***

VOLUME XXX (2011): **ISBN:** 978-981-08-9528-0

Editors

Dr C T Tam *(OWICS)*
Prof. K C G Ong *(NUS)*
Dr S Teng *(NTU)*
Prof. M H Zhang *(NUS)*

Conference Co-sponsors:

- BASF South East Asia Pte Ltd (*gold*)
- WAK Technologies Pte Ltd (*gold*)
- Unibeton Ready Mix, UAE
- Novaars International Pte Ltd
- Ready-Mixed Concrete Assn of Singapore
- Cement and Concrete Assn of Singapore
- Japan Concrete Institute

Organisers:

- CI-Premier Conference Organisation, Singapore

Conference Secretariat
CI-PREMIER PTE LTD
150 Orchard Road #07-14, Orchard Plaza
Singapore 238841
Tel: +65 67332922 Fax: +65 62353530
E-mail:ci-p@cipremier.com
Web: http://www.cipremier.com

FOREWORD

The 36th Conference on Our World in Concrete and Structures (OWICS11) is themed “Recent Advances in the Technology of Fresh Concrete”. This has always been a major area of focus in this series of conference. Over the years many papers have been presented in this area of concrete research. The intention this year is to bring together all those who share a common interest in this subject area to promote the sharing of new ideas and to sharpen the focus on the significant development and innovation that has taken place in recent years.

OWICS11 is also very special as we are dedicating it to Professor Olafur H Wallervick of the Innovation Centre Iceland for his support of this conference series and for his acknowledged contributions to concrete technology. He will deliver the OWICS11 Conference lecture.

The number of eminent and world renown speakers we have this year have exceeded all our expectations and I would like to thank all speakers, authors and participants for their contributions. Thanks are also due to the OWICS Honorary Chairmen, the OWICS Advisors, our Sponsors and the Organizing Committee.

Khim Chye Gary ONG
&
Min-Hong ZHANG
Conference Chairpersons

36th Conference on

Our World in Concrete & Structures

14 – 16 August 2011, Singapore

Volume XXX (2011): ISBN: 978-981-08-9528-0

Table of Contents

Special Papers Session in honour of Prof. O H Wallevik

OWICS Steering Council Keynote Papers

OW11 Keynote Papers

Technical Papers

Technical Papers

A Chapter on The Conceptual Approach to Structural Design

Keynote Papers

Technical Papers

INDEX OF AUTHORS

INDEX OF AUTHORS

For Link, please click on page numberrs

ISBN: 978-981-08-9528-0

SHEAR ANALYSIS OF REINFORCED CONCRETE SLABS WITH EFFECTIVE MOMENT OF INERTIA

Yu Liu*, Jimmy Chandra# and Susanto Teng#

*School of Civil & Environmental Engineeering
Nanyang Technological University
Blk N1, #50 Nanyang Avenue, Singapore 639798
e-mail: <cliuy@ntu.edu.sg> webpage: http://www.cee.ntu.edu.sg/

Keywords: Reinforced concrete slabs, Finite element analysis, Shear failure, Effective stiffness

Abstract. *The effective moment of inertia concept has been used to evaluate the bending stiffnesses of reinforced concrete (RC) members in design codes. Later, it was combined with finite element (FE) methods to calculate the deflection responses of RC slabs. However, the failure of the slabs cannot be predicted by the effective moment of inertia based method. In this work, an empirical failure criterion for RC slabs under bending and shear was adopted and modified to consider the stiffness degradation of shell elements in FE analysis. In order to predict the shear failure of the slabs, a softening curve for the bending and shear stiffnesses was proposed. The model parameters in the failure criterion were calibrated according to published test results. The comparison between the numerical and the experimental results shows that the proposed method can predict the deflection response and the shear strength of the analyzed slabs with acceptable accuracy.*

1 INTRODUCTION

The finite element (FE) analysis of reinforced concrete (RC) slabs is generally carried out by adopting either a layered element approach or an effective stiffness approach[1]. The layered approach divides the plate or shell elements into several layers through the thickness, and each layer has its own independent material properties. The layered plate or shell elements can be used to easily consider the nonlinear properties of concrete and the presence of steel reinforcements. Hence, their application in the FE analysis of RC slabs has been popular[2-4]. With the layered approach, one needs to call the constitutive model of concrete for each layer at each integration point of the elements. Hence, the analysis can be expensive and time consuming. Furthermore, the difficulties and complexities in modeling the concrete restrict the accuracy of the analysis results.

On the other hand, the effective stiffness approach[5-6] adopts an empirical effective bending stiffness of the element cross section to replace the iteration through the thickness for summing up the contributions of each layer. This approach can provide reasonable estimates of slab deflections in the early stage of loading. The computational cost is also much lower as compared with the layered method. However, the failure of the slabs cannot be predicted by using this method.

In this work, efforts have been made to predict the shear failure of reinforced concrete (RC) slabs through FE analysis using the effective stiffness approach. In the next section, the used

Nanyang Technological University, Singapore

finite element is described. Then, in Section 3, the material matrix based on the effective moment of inertial concept is derived. In order to predict the shear failure of the slabs, a softening curve for the bending and shear stiffnesses is also proposed based on an empirical failure criterion for RC slabs under bending and shear. Some numerical examples are worked out and compared with the experimental results in Section 4 and the paper is summarized in Section 5.

2 FINITE ELEMENT FORMULA

In this work, a 9-node heterosis shell element [7] is adopted. It had been modified to be a non-layered form[8]. In the non-layered shell element, the general strain vectors comprises of 8 component, i.e.,

$$\boldsymbol{\varepsilon} = \{\varepsilon_{0x} \quad \varepsilon_{0y} \quad \gamma_{0xy} \quad \gamma_{xz} \quad \gamma_{yz} \quad \varphi_x \quad \varphi_y \quad \varphi_{xy}\}^T \tag{1}$$

where ε_{0x}, ε_{0y} and γ_{0xy} are the in-plane strains at mid-plane ($z = 0$); γ_{xz} and γ_{yz} are the transverse shear stains; φ_x, φ_y and φ_{xy} are the curvatures. The new 8×45 geometric matrix which maps the general nodal displacements into the general strains, $\mathbf{B_n}$, was derived to replace the original 5×45 geometric matrices, $\mathbf{B}$, for the layered element where the general strain vectors include only 5 components (ε_x, ε_y, γ_{xy}, γ_{xz} and γ_{yz}).

The first 5 rows of $\mathbf{B_n}$ are the same as those of matrix $\mathbf{B}$ at mid-layer ($z = 0$). The last 3 rows of $\mathbf{B_n}$ are obtained from

$$\begin{Bmatrix} \varphi_x \\ \varphi_y \\ \varphi_{xy} \end{Bmatrix} = \begin{bmatrix} \partial_x & 0 \\ 0 & \partial_y \\ \partial_y & \partial_x \end{bmatrix} \cdot \begin{Bmatrix} \theta_x \\ \theta_y \end{Bmatrix} = \sum_{i=1}^{9} \begin{bmatrix} N_x^i & 0 \\ 0 & N_y^i \\ N_y^i & N_x^i \end{bmatrix} \cdot \begin{Bmatrix} \theta_x^i \\ \theta_y^i \end{Bmatrix} \tag{2}$$

where θ_x^i and θ_y^i ($i = 1\cdots9$) are the nodal rotation angles; N_x^i and N_y^i ($i = 1\cdots9$) are the partial derivatives of the shape functions N^i with respect to x and y, respectively. With material matrix, $\mathbf{D}$, and the geometric matrix, $\mathbf{B_n}$, the element stiffness matrix can be obtained by numerical integration as

$$\mathbf{K_e} = \iint_\Omega \mathbf{B_n}^T \cdot \mathbf{D} \cdot \mathbf{B_n} \cdot d\Omega \ . \tag{3}$$

The selective integration scheme is adopted in Eq.(3) to avoid the locking problem. The material matrix $\mathbf{D}$ is discussed in the next section.

3 MATERIAL MATRIX

3.1 Material matrix before cracking

For an orthotropic elastic plane stress problem, the stress-strain relationship is

$$\begin{Bmatrix} \sigma_x \\ \sigma_y \\ \tau_{xy} \end{Bmatrix} = \frac{1}{1-\nu_x\nu_y} \begin{bmatrix} E_x & \nu_y E_x & 0 \\ \nu_x E_y & E_y & 0 \\ 0 & 0 & (1-\nu_x\nu_y)G_{xy} \end{bmatrix} \begin{Bmatrix} \varepsilon_x \\ \varepsilon_y \\ \gamma_{xy} \end{Bmatrix}. \tag{4}$$

where E_x, ν_x and E_y, ν_y are the moduli and Poisson's ratios in x and y directions, respectively; G_{xy} is the shear modulus in x-y plane. In the shell element, the in-plane strains can be calculated from the curvatures and the mid-plane strains as

$$\begin{Bmatrix} \varepsilon_x \\ \varepsilon_y \\ \gamma_{xy} \end{Bmatrix} = \begin{Bmatrix} \varepsilon_{0x} \\ \varepsilon_{0y} \\ \gamma_{0xy} \end{Bmatrix} + \begin{Bmatrix} \varphi_x \\ \varphi_y \\ \varphi_{xy} \end{Bmatrix} z. \tag{5}$$

The in-plain forces are thus calculated as

$$\begin{Bmatrix} N_x \\ N_y \\ N_{xy} \end{Bmatrix} = \int_{-t/2}^{t/2} \begin{Bmatrix} \sigma_x \\ \sigma_y \\ \tau_{xy} \end{Bmatrix} dz = \frac{t}{1-\nu_x\nu_y} \begin{bmatrix} E_x & \nu_y E_x & 0 \\ \nu_x E_y & E_y & 0 \\ 0 & 0 & (1-\nu_x\nu_y)G_{xy} \end{bmatrix} \begin{Bmatrix} \varepsilon_{0x} \\ \varepsilon_{0y} \\ \gamma_{0xy} \end{Bmatrix} \tag{6}$$

where t is the thickness. The moments are obtained as

$$\begin{Bmatrix} M_x \\ M_y \\ M_{xy} \end{Bmatrix} = \int_{-t/2}^{t/2} \begin{Bmatrix} \sigma_x \\ \sigma_y \\ \tau_{xy} \end{Bmatrix} z dz = \frac{t^3/12}{1-\nu_x\nu_y} \begin{bmatrix} E_x & \nu_y E_x & 0 \\ \nu_x E_y & E_y & 0 \\ 0 & 0 & (1-\nu_x\nu_y)G_{xy} \end{bmatrix} \begin{Bmatrix} \varphi_x \\ \varphi_y \\ \varphi_{xy} \end{Bmatrix}. \tag{7}$$

The transverse shear forces-strain relationship is

$$\begin{Bmatrix} Q_x \\ Q_y \end{Bmatrix} = \int_{-t/2}^{t/2} \begin{Bmatrix} \tau_{xz} \\ \tau_{yz} \end{Bmatrix} dz = t \begin{bmatrix} G_{xz} & 0 \\ 0 & G_{yz} \end{bmatrix} \begin{Bmatrix} \gamma_{xz} \\ \gamma_{yz} \end{Bmatrix} \tag{8}$$

From Eqs.(6)-(8), the material matrix **D** is obtained as

$$\begin{Bmatrix} N_x \\ N_y \\ N_{xy} \\ Q_x \\ Q_y \\ M_x \\ M_y \\ M_{xy} \end{Bmatrix} = \begin{bmatrix} \frac{tE_x}{1-\nu_x\nu_y} & \frac{t\nu_y E_x}{1-\nu_x\nu_y} & 0 & 0 & 0 & 0 & 0 & 0 \\ \frac{t\nu_x E_y}{1-\nu_x\nu_y} & \frac{tE_y}{1-\nu_x\nu_y} & 0 & 0 & 0 & 0 & 0 & 0 \\ 0 & 0 & tG_{xy} & 0 & 0 & 0 & 0 & 0 \\ 0 & 0 & 0 & tG_{xz} & 0 & 0 & 0 & 0 \\ 0 & 0 & 0 & 0 & tG_{yz} & 0 & 0 & 0 \\ 0 & 0 & 0 & 0 & 0 & \frac{E_x t^3/12}{1-\nu_x\nu_y} & \frac{\nu_y E_x t^3/12}{1-\nu_x\nu_y} & 0 \\ 0 & 0 & 0 & 0 & 0 & \frac{\nu_x E_y t^3/12}{1-\nu_x\nu_y} & \frac{E_y t^3/12}{1-\nu_x\nu_y} & 0 \\ 0 & 0 & 0 & 0 & 0 & 0 & 0 & \frac{t^3 G_{xy}}{12} \end{bmatrix} \begin{Bmatrix} \varepsilon_{0x} \\ \varepsilon_{0y} \\ \gamma_{0xy} \\ \gamma_{xz} \\ \gamma_{yz} \\ \varphi_x \\ \varphi_y \\ \varphi_{xy} \end{Bmatrix} \tag{9}$$

Before cracking, the shell elements behave linearly, and

$$E_x = E_y = E_c, \quad \upsilon_x = \upsilon_y = \upsilon_c, \quad G_{xy} = G_{xz} = G_{yz} = G_c = \frac{E_c}{2(1+\upsilon_c)} \tag{10}$$

where E_c and υ_c are the modulus and the Poisson's ratio of the concrete, respectively.

3.2 Stiffness reduction factors

After cracking, the stiffnesses of the shell element, in Eq.(9), will degrade. Polak[5] and Vecchio & Tata[6] defined the stiffness reduction factors α_x and α_y to consider the concrete cracking induced stiffness degradation in the x- and y- directions, respectively. The stiffness reduction factors α_x and α_y were defined based on the concept of effective moment of inertia, which is calculated as,

$$I_e = \left(\frac{M_{cr}}{M^e}\right)^a I_g + \left[1 - \left(\frac{M_{cr}}{M^e}\right)^a\right] I_{cr} \tag{11}$$

where $M_{cr} = \frac{f_r I_g}{y_t}$ is the cracking moment; $f_r = 0.6\sqrt{f_c'}$ is the modulus of rupture of the concrete; y_t is the distance from neural axis to the tension face of the uncracked section; I_g is the gross moment of inertia; I_{cr} is the moment of inertia of the fully cracked cross section; M^e is the elastic bending moment; and $a = 3$.

Given the details of the element's cross sections in x- and y- directions and the current general strain vector, the effective moment of inertias in x- and y- directions, I_{ex} and I_{ey}, can be calculated. To account for the torsional moment, M_{xy}, in the shell elements, the elastic bending moment, M^e, in Eq.(11), was suggested to be replaced by a generalized moment, $\widetilde{M}^e$, as

$$\widetilde{M}_x^e = |M_x^e| + |M_{xy}^e|, \quad \widetilde{M}_y^e = |M_y^e| + |M_{xy}^e| \tag{12}$$

where the elastic moments M_x^e, M_y^e and M_{xy}^e are calculated from Eq.(9) when Eq.(10) is used. The stiffness reduction factors α_x and α_y were thus defined as,

$$\alpha_x = I_{ex}/I_{gx}, \qquad \alpha_y = I_{ey}/I_{gy} \tag{13}$$

Finally, the concrete cracking induced stiffness degradation of the shell elements is taken into account by α_x and α_y, and Eq.(10) is updated as

$$\begin{gathered} E_x = \alpha_x E_c, \quad E_y = \alpha_y E_c, \quad \upsilon_x = \alpha_x \upsilon_c, \quad \upsilon_y = \alpha_y \upsilon_c \\ G_{xy} = \alpha_x \alpha_y G_c, \quad G_{xz} = \alpha_x G_c, \quad G_{yz} = \alpha_y G_c \end{gathered} \tag{14}$$

It has been shown that with Eq.(14), the reasonably good estimates to the deflection of RC slabs under service load level can be achieved[6].

3.3 Modified stiffness reduction factors

To predict the failure of the analyzed slabs, we need to account for the further degradation of the stiffnesses due to steel yielding and shear failure of the concrete. In this work, an empirical failure criterion for RC slabs subjected to shear and bending by Yamada et. al.[9] is used, i.e.,

$$\left(\frac{M/M_n}{1.43}\right)^2 + \left(\frac{V/V_n}{1.43}\right)^2 = 1 \tag{15}$$

where M_n and V_n are the bending moment capacity and the shear capacity of the considered slab, respectively. To measure the further stiffness degradation of the shell elements, a factor R is defined, similar to Eq.(15), as

$$R = \left(\frac{M/M_n}{C_M}\right)^2 + \left(\frac{Q/Q_n}{C_Q}\right)^2 \tag{16}$$

where C_M and C_Q are model parameters which will be discussed in the next section. The bending moment capacity of the considered cross section can be calculated as

$$M_n = \rho d f_y j_d \tag{17}$$

where ρ is the tension steel reinforcement ratio; d is the effective depth of slab; f_y is the yielding strength of the tension steel; and j_d is the distance from the tension steel to the resultant compressive force of the cross section. The shear capacity is calculated using the empirical formula[10], i.e.,

$$Q_n = 59t\left[f_c'(\rho + \rho')\frac{Qd}{M}\right]^{1/3} + d\rho_w f_{y1} \tag{18}$$

where ρ' is the compression steel reinforcement ratio; f_c' is the compressive strength of concrete in psi; ρ_w is the shear steel reinforcement ratio; and f_{y1} is the yielding strength of the shear steel.

During FE analysis, the factors used to measure the further stiffness degradation in x- and y-directions, R_x and R_y, can be calculated according to Eqs.(16)-(18). The modified stiffness reduction factors are then defined as

$$\alpha_x' = \alpha_x/(1 + R_x), \quad \alpha_y' = \alpha_y/\left(1 + R_y\right) \tag{19}$$

In this work, the stiffness reduction factors α_x and α_y in Eq.(14) are replaced by the modified factors α_x' and α_y' in Eq.(19). The softening caused by steel yielding and shear failure of the concrete is thus taken into account.

4 NUMERICAL EXAMPLES

The material matrix discussed above has been implemented as a user defined material in the finite element analysis program FEAP[11]. The secant stiffness scheme is adopted in the computation. The model parameters C_M and C_Q in Eq.(16) are chosen as 3.3 and 1.6 by trial and error method. Three serieses of slabs are analysed and the obtained results are compared with the test results. The first and the second serieses include four slabs tested at Talbot laboratory, University of Illinois by Elstner and Hognestad[12]. The third series includes five slabs tested at research and development laboratory of Portland Cement Association also by Elstner and Hognestad[12].

4.1 Slabs supported on four edges with corners free to lift (Series II)[12]

The series II of the experiment involved 3 panels of 152.4mm thick slabs loaded monolithically through 356mm column stubs. The slabs were simply supported at four edges with the corners free to lift. The slab details are shown in Table 1.

Specimen	Dimensions (mm)	Depth (mm)	Concrete		Reinforcement		
			f'_c (MPa)	E_c (MPa)	f_y (MPa)	ρ' %	ρ %
A-4	1828.8 × 1828.8 × 152.4	117.6	26.2	24449	332.7	0.6	1.2
A-5	1828.8 × 1828.8 × 152.4	114.3	27.8	25212	321.7	1.2	2.5
A-6	1828.8 × 1828.8 × 152.4	114.3	25.1	23947	321.7	1.2	3.7

Table 1: Details of slabs in series II

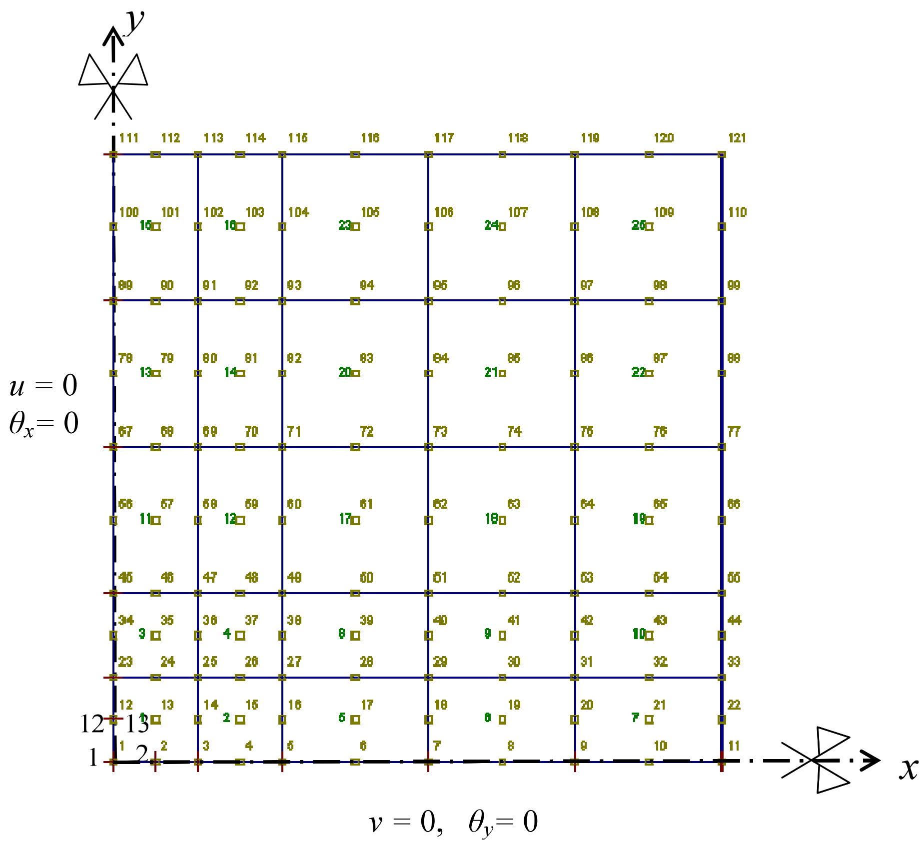

Figure 1: Computational modelling of slabs

A quarter of slab is modelled using 121 nodes and 25 elements as shown in Figure 1. The loadings were applied equally at nodes 1, 2, 12 and 13 (position of column stud). Since only a quarter of slab is modelled, the rotation angle θ_y, and the displacement v of the boundary nodes on line $y = 0$ are zeros, because of symmetry. The rotation angle θ_x, and the displacement u of the boundary nodes on line $x = 0$ are also zeros. The obtained results of load versus central deflection curves are plotted in Figure 2 together with the test results. The typical deflection distributions at the early stage and the near failure stage are shown in Figure 3. From Figure 3b, the deformation localization close to the column can be observed, which indicates that a punching shear failure has happened. The numerical results are generally agreeable with the experimental results.

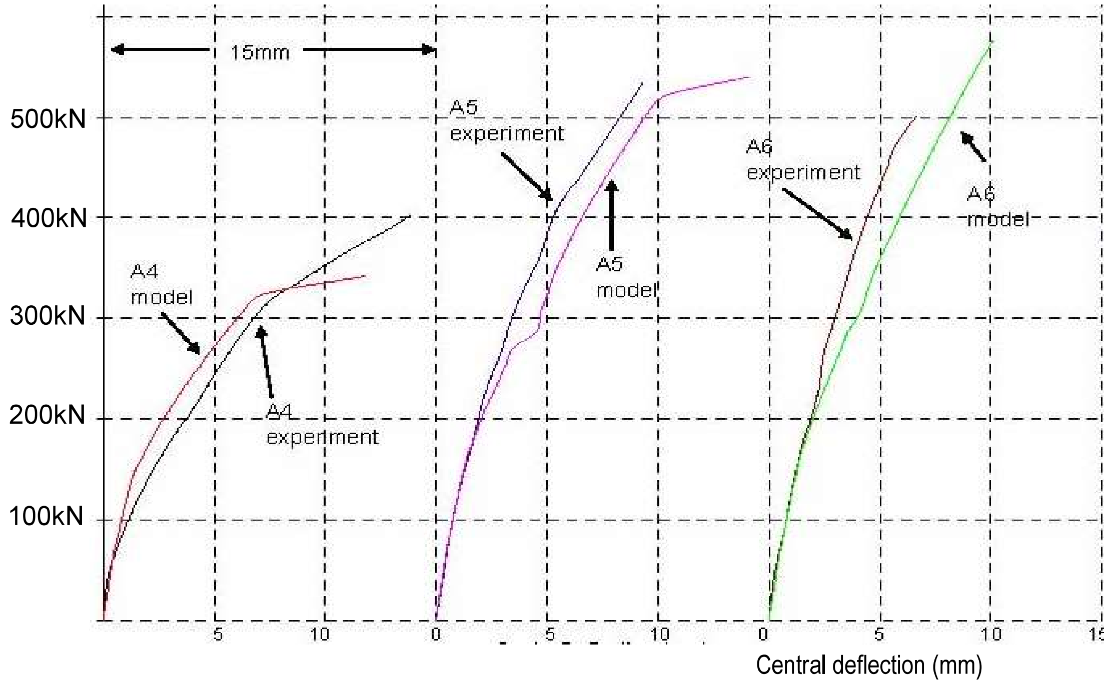

Figure 2: Load-central deflection curves of slabs in series II

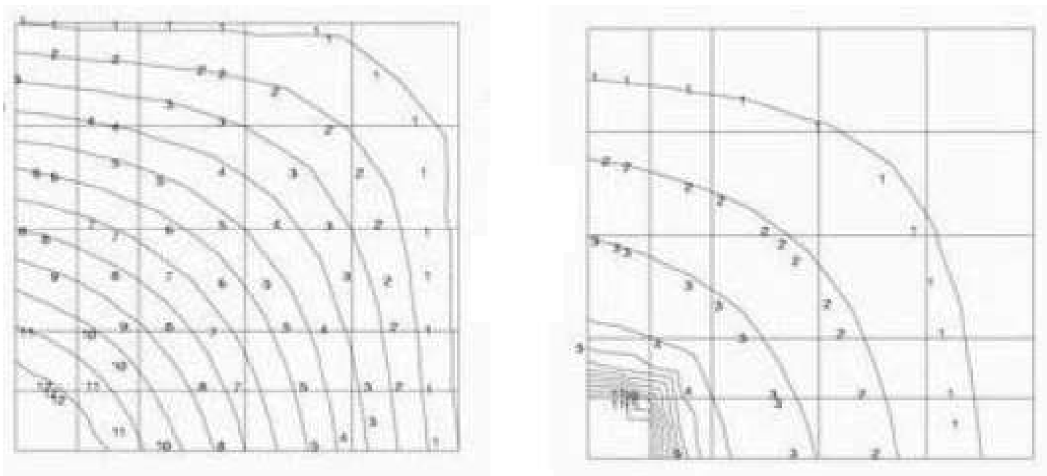

a. Deflection distribution at early stage b. Deflection distribution near failure

Figure 3: Typical deflection distributions

4.2 Slabs supported at four corners (Series IV)[12]

The series IV involves one slab supported on four corners and loaded through a 254mm column stub. The details of the slab are shown in Table 2. Similarly, a quarter of the slab is modelled with 121 nodes and 25 elements and the symmetric boundary conditions are applied to the nodes on lines $x = 0$ and $y = 0$. The obtained load versus central deflection curve are plotted and compared with the test result in Figure 4. The predicted strength conforms to the experimental result while the predicted central deflection is larger than the experimental observation.

Specimen	Dimensions (mm)	Depth (mm)	Concrete		Reinforcement		
			f'_c (MPa)	E_c (MPa)	f_y (MPa)	ρ'%	ρ%
A7a	1828.8 × 1828.8 × 152.4	114.3	28.5	25293	321.7	1.2	2.5

Table 2 Details of slab A7a in series IV

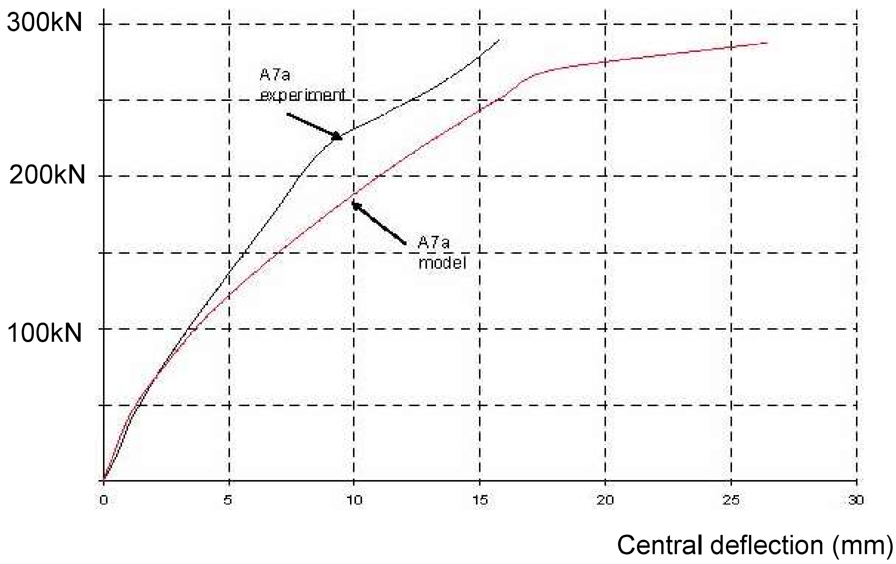

Figure 4: Load-central deflection curves for slab in series IV

4.3 Slabs supported on four edges with corners free to lift (Series VIII)[12]

In this work, 5 slabs in series VIII are also selected to analysis. They are loaded through 254mm column stubs, and simply supported at four edges with the corners free to lift. There is no compression steel and the tension steel reinforcement ratios range from 0.5% to 3.0%. For the slab DEH B12, two rows of vertical stirrup with cross sectional area of 1419mm^2 were used, and the shear reinforcement ratio is about 0.57%. The slab details are shown in Table 3. Again, a quarter of the slab is modelled with 121 nodes and 25 elements and the symmetric boundary conditions are applied at lines $x = 0$ and $y = 0$. The obtained load versus central deflection curves are compared with the test results in Figure 5.

Specimen	Dimensions (mm)	Depth (mm)	Concrete		Reinforcement		
			f'_c (MPa)	E_c (MPa)	$f_y = f_{y1}$ (MPa)	ρ_w %	ρ %
DEH B02	1828.8 × 1828.8 × 152.6	114.3	47.6	32978	320.6	-	0.5
DEH B04	1828.8 × 1828.8 × 152.6	114.3	47.7	33013	303.4	-	1.0
DEH B09	1828.8 × 1828.8 × 152.6	114.3	43.9	31670	341.3	-	2.0
DEH B14	1828.8 × 1828.8 × 152.6	114.3	50.5	33968	325.4	-	3.0
DEH B12	1828.8 × 1828.8 × 152.6	114.3	45.9	32384	331.6	0.57	3.0

Table 3 Details of slabs in series VIII

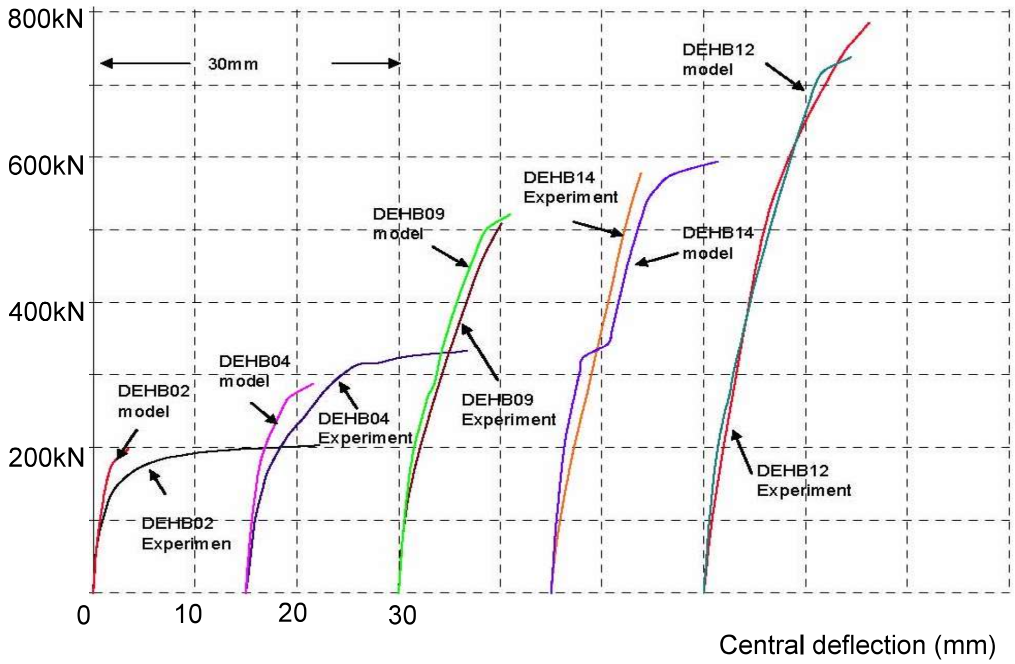

Figure 5 Load-central deflection curves for slab in series VIII

In experiment, slabs B09, B12 and B14 are observed to fail by punching shear. The predicted strengths and central deflections generally agree with the test results. For slabs B02 and B04, the numerical results still suggest a shear failure; however, they are actually failed by flexure in the experiment. It shows that, the proposed method maybe only applicable for the slabs subjected to shear failure

5 CONCLUSIONS

In this work, efforts have been made to predict the failure of RC slabs using the FE analysis based on the effective stiffness approach. The non-layered form of the 9-node heterosis shell element is used and the degradation of material matrix due to concrete cracking is reflected by the stiffness reduction factors. In order to predict the failure of the slabs, a softening curve for the bending and shear stiffnesses was proposed based on an empirical failure criterion for RC slabs under bending and shear. The stiffness reduction factors defined by Polak[5] are modified accordingly to consider the further degradation of the stiffnesses due to steel yielding and shear failure of the concrete. The model parameters C_M and C_Q in the softening curve are set to be 3.3 and 1.6, respectively, by trial and error method. Three series of RC slabs were analysed using the proposed method. The computed deflection responses and shear strengthes are agreeable with the test results for the slabs subjected to shear failure. Further work is needed to predict the deflection and the strength of slabs subjected to flexure.

REFERENCES

[1] J. Jiang and F. A. Mirza, “Nonlinear analysis of reinforced concrete slabs by a discrete finite element approach”, *Computers and Structures*, 65(4), 585-592, (1997).

[2] H.W. Song, S.H. Shim and K.J. Byun, “Failure analysis of reinforced concrete shell structures using layered shell element with pressure node”, *ASCE Journal of Structural Engineering*, 128(5), 655-664, (2002).

[3] S. Teng, Y. Liu and C.K. Soh, “Flexural analysis of reinforced concrete slabs using degenerated shell element with assumed strain and 3-D concrete model”, *ACI Structural Journal*, 102(4), 515-525, (2005).

[4] W.Y. Wang and S. Teng, “Finite-element analysis of reinforced concrete flat plate structures by layered shell element.” *ASCE Journal of Structural Engineering*, 134(12), 1862-1872, (2008).

[5] M.A. Polak “Effective stiffness model for reinforced concrete slabs”, *ASCE Journal of Structural*

Engineering, 122(9), 1025-1030,(1996).
[6] F.J. Vecchio and M. Tata, “Approximate analysis of reinforce concrete slabs”, *Structural Engineering and Mechanics*, 8(1), 1-18, (1999).
[7] E. Hinton and D.R.J. Owen, *Finite Element Software for Plates and Shells*, Pineridge Press, Swansea, U.K. (1984).
[8] Y. Liu and S. Teng, “Nonlinear analysis of reinforced concrete slabs using nonlayered shell element”, *ASCE Journal of Structural Engineering*, 134(7), 1092-1100, (2008).
[9] T. Yamada, A. Nanni and K. Endo, “Punching shear resistance of flat slabs: influence of reinforcement type and ratio”, *ACI Structural Journal*, 88(4), 555-563, (1992).
[10] ASCE-ACI Committee 445 on Shear and Torsion, “Recent approach to shear design of structural concrete”, *ASCE Journal of Structural Engineering*, 124(12), 1375-1404, (1998).
[11] R.L. Taylor *FEAP--A Finite Element Analysis Program, V7.4 programmer manual*, Univ. of California at Berkeley, (2001).
[12] R.C. Elstner and E. Hognestad, “Shearing strength of reinforced concrete slabs,” *ACI Journal Proceedings*, 53(1), 29-58, (1956).

- Word Count: 2458

Plagiarism Percentage

17%

sources:

1 6% match (publications)
Liu, Yu, and Susanto Teng. "Nonlinear Analysis of Reinforced Concrete Slabs Using Nonlayered Shell Element", Journal of Structural Engineering, 2008.

2 3% match (Internet from 03-Nov-2012)
http://www.demoforests.net/Warehouse/Docs/Other/Wensel/CACTOS/Note6.pdf

3 2% match (Internet from 09-Mar-2016)
http://ir.canterbury.ac.nz/bitstream/handle/10092/6410/dann_thesis.pdf?isAllowed=y&sequence=1

4 2% match (Internet from 08-Feb-2014)
http://kurskservice.ru/2011-06-19-16-54-17/63-bonus.pdf

5 2% match (Internet from 02-Jul-2013)
http://svn.gna.org/svn/freeciv/tags/R1_14_1/data/misc/intro.xpm

6 2% match (Internet from 20-Oct-2013)
http://www2.americanexpress.ro/Amex/pdf/ro/AMEX%2013%2002%202013.xls

7 1% match (Internet from 07-Feb-2014)
http://66.180.169.221/pdf/314.pdf

paper text:

finite element is described. Then, in Section 3, the material matrix based on the effective moment of inertial concept is derived. In order to predict the shear failure of the slabs, a softening curve for the bending and shear stiffnesses is also proposed based on an empirical failure criterion for RC slabs under bending and shear. Some numerical examples are worked out and compared with the experimental results in Section 4 and the paper is summarized in Section 5. 2 FINITE ELEMENT FORMULA In this work, a 9-node heterosis shell element 7 is adopted. It had been modified to be a non- layered form8. In the non-layered shell element, the general strain vectors comprises of 8 component, i.e., (1) where E0,, E0, and Yo,, are the in-plane strains at mid-plane (z = O); Yu and y,. are the transverse shear stains; ,p,, ,p, and ,p.,, are the curvatures. The new Bx45 geometric matrix which maps the general nodal displacements into the general strains, Bn, was derived to replace the original 5x45 geometric matrices, B, for the 1

layered element where the general strain vectors include only 5 components (e, e,., y.,,, Yu and y,.). The first 5 rows of Bn are the same as those of matrix B at mid-layer

(z = 0). The last 3 rows of Bn are obtained from 1

[mY<<.piz>y,,) [acl0, clo] {00"} = ,'_,[NN0'! oNN;,':] ·{: "} (2) = , · y x y where 8' and 91 (i = I··9) are the nodal rotation angles; N' and N' (i = 1..·9) are the partial % y x y

derivatives of the shape functions N ; with respect to x and y, respectively. 1

With

material matrix, D, and the geometric matrix, B., the element stiffness matrix can be 1

obtained by numerical integration as K• = ffB•r ·D· B • ·dQ . (3) The

selective integration scheme is adopted in Eq.(3) to avoid the locking problem. 1

The material " matrix D is discussed in the next section. 3 MATERIAL MATRIX 3.1 Material matrix before cracking For an orthotropic elastic plane stress problem, the stress-strain relationship is QO] {Exy J . (4) (1 - vxvy)Gxy Yxy where E,, v, and E,, v,are the moduli and Poisson's ratios in x and y directions, respectively; G,,is the shear modulus in x-y plane. In the shell element, the in-plane strains can be calculated from the curvatures and the mid-plane strains as {YEExyxy} = {YEoooxyxyJ + {<(<(JffJJyxxyJ z. (5) 4.1 Slabs supported on four edges with corners free to lift (Series II)12 The series II of the experiment involved 3 panels of 152.4mm thick slabs loaded monolithically through 356mm column stubs. The slabs were simply supported at four edges with the corners free to lift. The slab details are shown in Table 1. Specimen Dimension Dept Concrete Reinforcement s (mm) h f'c(MPa) Ee (MPa) f,(MPa) p' % p % 1(m17m.6) A-4 1828.8 x 1828.8 x 152.4 26.2 24449 332.7 0.6 1.2 A-5 1828.8 x 1828.8 x 152.4 114.3 27.8 25212 321.7 1.2 2.5 A-6 1828.8 x 1828.8 x 152.4 114.3 25.1 23947 321.7 1.2 3.7 Table 1: Details of slabs in series II 1 _,,_.'+-+- -+- 1-- -i- -+"- ·- ·x v = 0, 8y= 0 Figure 1: Computational modelling of slabs A quarter of slab is modelled using 121 nodes and 25 elements as shown in Figure 1. The loadings were applied equally at nodes 1, 2, 12 and 13 (position of column stud). Since only a quarter of slab is modelled, the rotation angle By. and the displacement v of the boundary nodes on line y = o are zeros, because of symmetry. The rotation angle 8,, and the displacement u of the

1

boundary nodes on line x = o are also zeros. The

1

obtained

results of load versus central deflection curves are plotted in Figure 2 together with the test results. The

1

typical deflection distributions at the early stage and the near failure stage are shown in Figure 3. From Figure 3b, the deformation localization close to the column can be observed, which indicates that a punching shear failure has happened. The numerical results are generally agreeable with the experimental results. 500kN 400kN 300kN 200kN 100kN - ----

r-- -- - -r-- - - - -r- - - - - -r- - - -- -,-- -- -r- -- - - -1- - - - - -,- - - ---· . . . . 1I 15mm I I 1 I 1 I 1 I 1 I / 1 I I I

5

I I I I I I I I I I I I I I I I ----- ----- ----- 5---- --- r-----------:----'--:------: , , , experiment , A,1 , / , • I I I I "I I I I - -- -- - -- -- - 7- - --- - - - - - -- --e -X' pe riment ,:r/---; o$•e,- -- -:•I , , , , I I I f , I I I : A5 : : J : : i -- I

6

0_ct =' -- -- - --ri- - - --

-I-- - ---I I I I I I \ I I I I I I I I I I I I I I I - -_M__

5

_----- -------------- .--_:__---_:_--___: : expe ment : : : : : : : _ _ _ _

LI _ _ _ _ _ LI _ _ _ _ _ IL _ _ _ _ LI _ _ _ _ _ LI _ _ _ _ _ LIL,_ _ _ _ LI _ _ _ _ JI_ _ _ _ _ JI I I I I I I I I I I I I I I I I; I I I I I I I I I I I I I I I I I I I I

4

_ _ _ _ _IL_ _ _ _ _IL_ _ _ _ _ _ _ _ _ _LI _ _ _ _ _LI _ _ _ _ _ L _ _ _ _ _LI _ _ _ _ _LI _ _ _ _ _,I 5 10 0 • . 5 _ • .• 1(! 0 5 10 1t CenlJal deflection (mm) Figure 2:Load-centraldeflection curves of slabs in series II a. Deflection distribution at early stage b.Deflection distribution near failure Figure 3:Typical deflection dsitributions 4.2 Slabs supported at four corners (Sarin IV)12 The series IV involves one slab supported on four corners and loaded through a 254mm coulmn stub. The detasli of the slab are shown in Table 2. Similarly,

a quarter of the slab is modeled 1

with "121nodes and 25 elements and the symmetric boundary conditions are applied to the nodes on lines test resultni Figure 4. The predicted strength confonns to the experimentalresult whilethe predicted = o andy = o. The obtainedolad versus centraldeflection curve are plotted and compared with the centraldeflection islarger thanthe experimentalobservation. Specimen Dimensions (mm) Depth (mm) fe(MPa) Concrete Ee (MPa) /y (MPa) Reinforcement p 'o/o p% A7a 1828.8 x 1828.8 x 152.4 114.3 28.5 25293 321.7 1.2 2.5 300kN 200kN 100kN Table 2 Details of slab A7a in series IV ------------ II1IIII:I-_--A-_e-7xpAa-er-itn-e.-nL,I:I-IIII---,-;-/-/-.III-_-_-_---_--_--:I-rI-II-----------------I;,-----:-I-II--II I : 7 I I A7- - r -- --- 1 ______ J _ --------a _ L _ _ _ _ _ _ J _ _ _ _ _ _ _ L_ _ _ _ _ _ J model 1 , I I I I -4I------ I-------I ------4I------- I ------1I I I I I I I I I I I - ----4I------ I-------I ------4I-------I ------ I I I I I I I I I I I 0 5 10 15 20 25 3) Centraldeflection (mm) Figure 4: Load-centraldeflection curves for slab in series VI 4.3 Slabs supported on four edga with comers free to lift (SarinVlll)12 nI this work, 5 slabs in series VIII are also selected to anaylsis. They are loaded through 254mm column stubs, and simply supported at four edges with the comers free to lift. There si no compression steeland the tension steel reinforcement ratios range from 0.5% to 3.0%.For the slab DEH 812, two rows of verticalstinup with cross sectionalarea of 1419mm2 were used, and the shear reinforcement ratio is about 0.57%. The slab details are shown in Table 3. Again, a quarter of the slabis modelled with 121 nodes and 25 elements and the symmetric boundary conditions are applied at lines x = o and>' = o. The obtained load versus centraldeflection curves are compared with the test results in Figure 5. Specimen Dimensions Depth Concrete Reinforcement (mm) (mm) f 'e (MPa) E.,(MPa) Jy = fy, (MPa) p.,% p % - DEHB02 1828.8 x 1828.8 x 152.6 114.3 47.6 32978 320.6 0.5 - DEHB04 1828.8 x 1828.8 x 152.6 114.3 47.7 33013 303.4 1.0 - DEH 809 1828.8 x 1828.8 x 152.6 114.3 43.9 31670 341.3 2.0 - DEH B14 1828.8 x 1828.8 x 152.6 114.3 50.5 33968 325.4 3.0 DEH 812 1828.8 x 1828.8 x 152.6 114.3 45.9 32384 331.6 0.57 3.0 Table 3 Details of slabs in series VIII 800kN - - - - - 1- - - - - ""t - - - - - ""1 - - - - - - ---1 - - - - - -i- - - - - - r- - - - - - I - - - - - I -------1 -1 30mm

I : I : I I : -, I : I J j j mCDdel '- I I o¢HB12 I : I : I t : t - - - - - +- - - - - - -+ - - - - - --I - - - - - -1- - - - - -j - - - - - - I- - - - - t- - - - - + --------------------------I 600kN J I I I J I I I I I I I I I I t I I I I I I t I I I I I I I I ----- -----+ ----- ----- ----- ------ ---- -----+ ----- : : : : DEHB14 : : : 1 3

1 1 , Experiment , 1 1 1 DEHB09 1 1 1 1 ----- -- --- - --- mqcte1--- - , -- --- I - - - - - - -L - - - - - 400kN _____L ______.1_______ 7

J___

I I I I I I I _ _I_ _ _ _ _ _I _ _ _ _ _ L _ _ _ _ _ L ----- ----- I I I I t 200k N I I I I I 2

DEHB04 1 I -D-EHso / -moael - -1 - - I model , I I I I I I I t I I I t I I I t ll _______I _

___LI _____ I ______Jt I I I I t I I I I t I I I I t I I I I l -:------: \DEH12----:----- : 1 :

Expeiment : : --- --, -- - --I------ ----- I ----- TI -------------------------I Experirnen -------- -- ---

-- ---------I--------- -------I------I-----

t 0 10 20 30 Central deflection {mm) Figure 5 Load-central deflection curves for slab in series VIII In experiment, slabs 809, 812 and 814 are observed to fail by punching shear. The predicted strengths and central deflections generally agree with the test results. For slabs 802 and 804, the numerical results still suggest a shear failure; however, they are actually failed by flexure in the experiment. It shows that, the proposed method maybe only applicable for the slabs subjected to shear failure 5 CONCLUSIONS In this work, efforts have been made to predict the failure of RC slabs using the FE analysis based on the effective stiffness approach. The non-layered form of the 9-node heterosis shell element is used and the degradaiton of material matrix due to concrete cracking is reflected by the stiffness reduction factors. In order to predict the failure of the slabs, a softening curve for the bending and shear stiffnesses was proposed based on an empirical failure criterion for RC slabs under bending and shear. The stiffness reduction factors defined by Polak5 are modified accordingly to consider the further degradation of the stiffnesses due to steel yielding and shear failure of the concrete. The model parameters CM and CQ in the softening curve are set to be 3.3 and 1.6, respectively, by trial and error method. Three series of RC slabs were analysed using the proposed method. The computed deflection responses and shear strengthes are agreeable with the test results for the slabs subjected to shear failure. Further work is needed to

predict the deflection and the strength of slabs 1

subjected to flexure. REFERENCES

[1] J. Jiang and F. A. Mirza, "Nonlinear analysis of reinforced concrete slabs by a discrete finite element approach", Computers and Structures, 65(4), 585-592, (1997). [2] H.W. Song, S.H. Shim and K.J. Byun, "Failure analysis of reinforced concrete shell structures using layered shell element with pressure node", ASCE Journal of Structural Engineering, 128(5), 655-664, {2002). [3] S. Teng, Y. Liu and C.K. Soh, "Flexural analysis of reinforced concrete slabs using degenerated shell element with assumed strain and 3-D concrete model", AC/ Structural Journal, 102(4), 515-525, (2005). [4] W.Y. Wang and S. Teng, "Fintie-element analysis of reinforced concrete flat plate structures by layered shell element." ASCE Journal of Structural Engineering, 134(12), 1862-1872, (2008). [5] M.A. Polak "Effectvie stiffness model for reinforced concrete slabs", ASCE Journal of Structural Y. Liu, J. Chandra and S. Teng Y. Liu, J. Chandra and S. Teng Y. Liu, J. Chandra and S. Teng Y. Liu,J. Chandra and S. Teng Y. Liu, J. Chandra and S. Teng 313 31 4 31 5 31 6 31 7 31 8 31 9 320 321